Supplemental Information for:

Localization of anionic phospholipids in *Escherichia coli* cells

Piercen M. Oliver,[a] John A. Crooks,[a] Mathias Leidl,[b] Earl J. Yoon,[a] Alan Saghatelian,[b] and Douglas B. Weibel[a,c,d]#

Department of Biochemistry, University of Wisconsin-Madison, Madison, WI[a];
Department of Chemistry and Chemical Biology, Harvard University, Cambridge, MA[b];
Department of Chemistry, University of Wisconsin-Madison, Madison, WI[c];
Department of Biomedical Engineering, University of Wisconsin-Madison, Madison, WI[d]

#Author to whom correspondence should be addressed
Douglas B. Weibel
Departments of Biochemistry, Chemistry, and Biomedical Engineering
440 Henry Mall
Madison, WI 53706
United States
Phone: (608) 890-1342
E-mail: weibel@biochem.wisc.edu

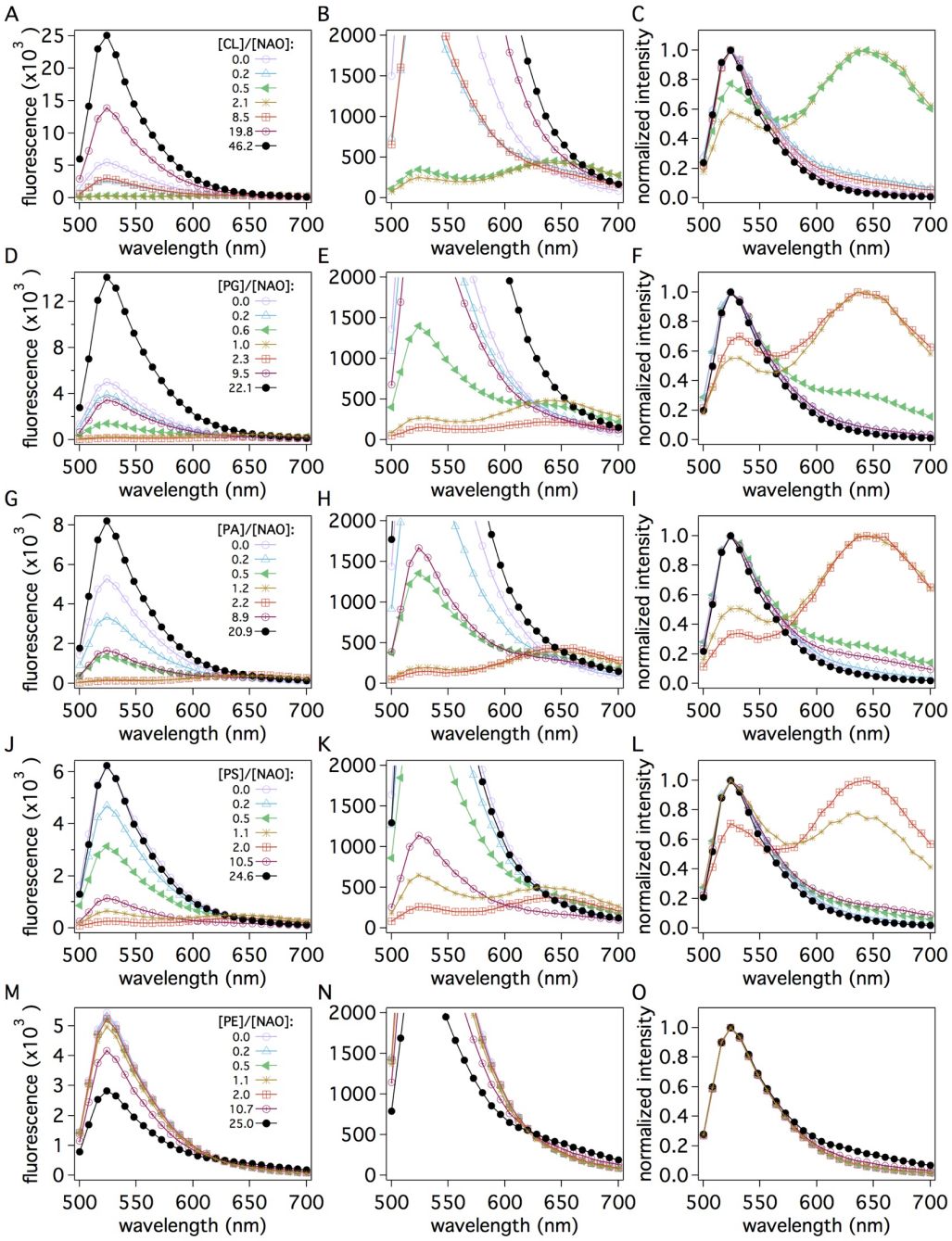

Figure S1. Fluorescence emission spectra of liposomes mixed with increasing concentrations of NAO. (A, D, G, J, M) Fluorescence versus wavelength spectra of NAO at seven concentrations of CL, PG, PA, PS, and PE, respectively. (B, E, H, K, N) Expanded view of the spectra immediately to the left. (C, F, I, L, O) Spectra (from the left) normalized to a maximum intensity of 1. NAO concentration is 5 μM in 10 mM Tris buffer, pH 8. Excitation is at a wavelength of 456 nm.

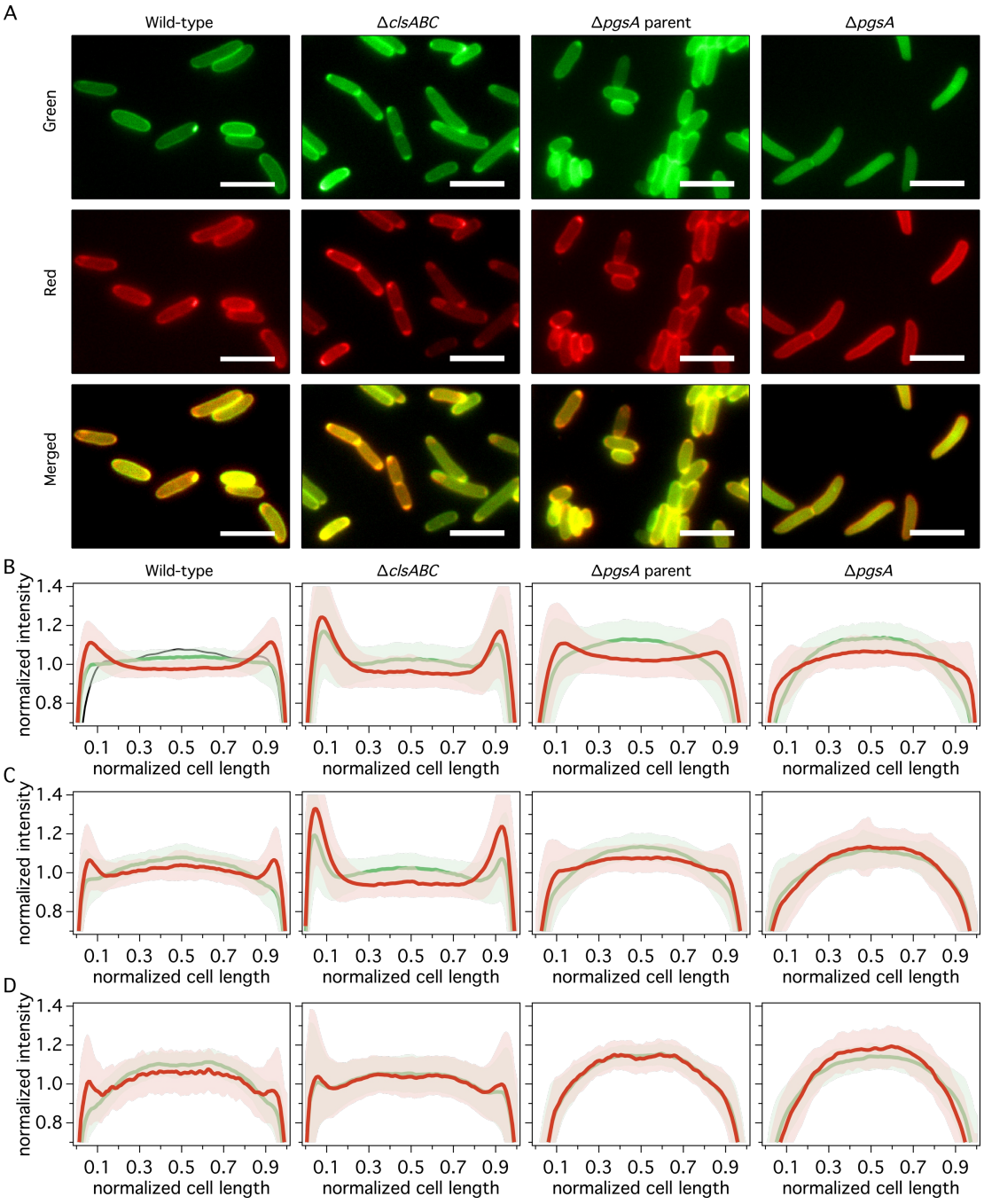

Figure S2. Comparison of green and red fluorescence emission of *E. coli* cells labeled with NAO. (A) Representative images of wild-type (MG1655), Δ*clsABC* (MG1655 BKT12), Δ*pgsA* parent (UE53), and Δ*pgsA* (UE54) *E. coli* cells labeled with 2 μM NAO and cultured at 30 °C to OD = 0.55 (λ = 600 nm, see Materials and Methods for details). Green and red channels are shown for each mutant, along with a merged image. The brightness of each channel in the merged images was altered until some yellow color was visible. Scale bars represent 5 μm. (B-D) Averaged intensity profiles of cells labeled with NAO versus the normalized cell length at concentrations of (B) 2 μM, (C) 1 μM, and (D) 0.5 μM NAO. The intensities along the long-axis of each cell were normalized to an area of 1 and averaged (N=166 to 733). The averages in the red channel are shown in red and green in green. The solid black line in (B) shows the average line profile from staining 198 wild-type cells with FM4-64. The shaded space surrounding the NAO fluorescence intensity profiles designates the standard error in the intensity at each point. Septating cells were intentionally left out of the analysis.

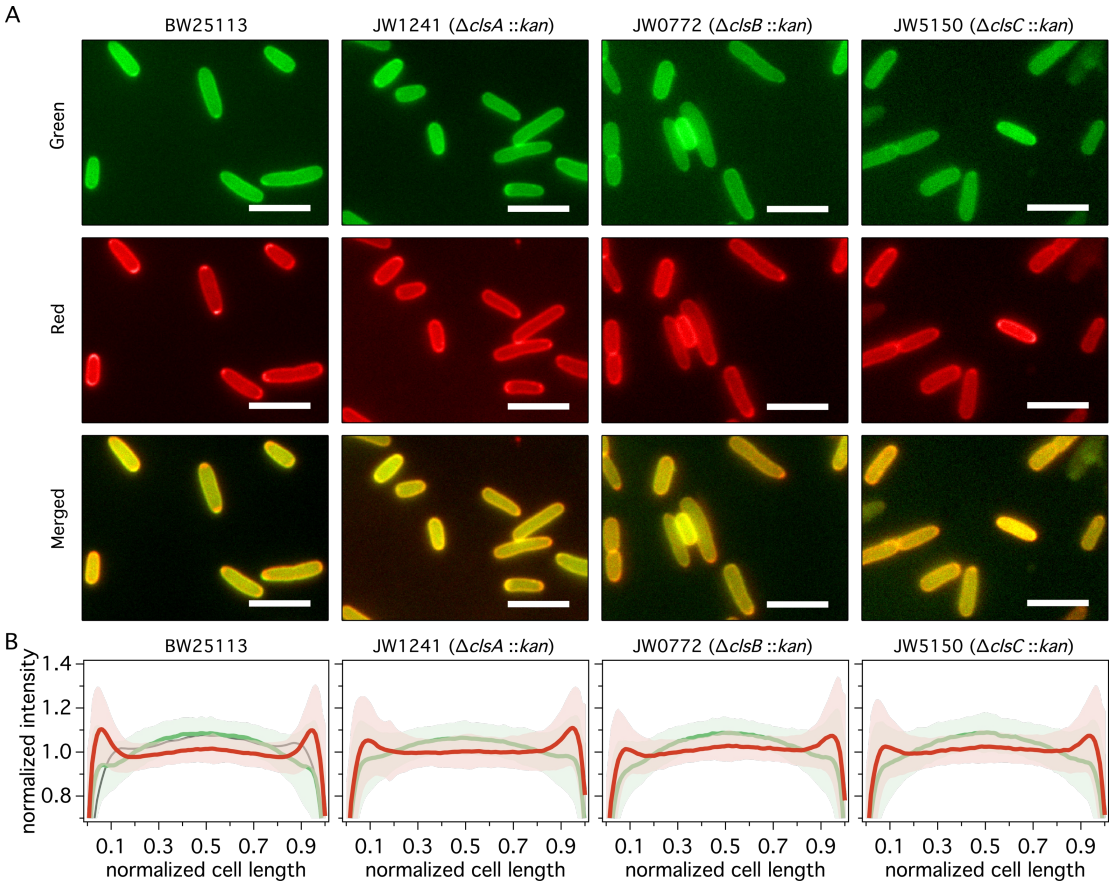

Figure S3. Comparison of green and red fluorescence emission of *E. coli* cells labeled with NAO from the Keio collection.[1] (A) Representative images of wild-type (BW25113), Δ*clsA* (JW1241), Δ*clsB* (JW0772), and Δ*clsC* (JW5150) *E. coli* cells labeled with 2 μM NAO and cultured at 30 °C to OD = 0.55 (λ = 600 nm, see Materials and Methods for details). Green and red channels are shown for each mutant, along with a merged image. The brightness of each channel in the merged images was altered until some yellow color was visible. Scale bars represent 5 μm. (B-D) Averaged intensity profiles of cells labeled with NAO versus the normalized cell length at a concentration of 2 μM NAO. The intensities along the long-axis of each cell were normalized to an area of 1 and averaged (N=246 to 492). The averages in the red channel are shown in red and green in green. The solid black line in (B) shows the average line profile from staining 198 wild-type (MG1655) cells with FM4-64. The shaded space surrounding the NAO fluorescence intensity profiles designates the standard error in the intensity at each point. Septating cells were intentionally left out of the analysis.

[1] **Baba T, Ara T, Hasegawa M, Takai Y, Okumura Y, Baba M, Datsenko KA, Tomita M, Wanner BL, Mori H.** 2006. Construction of *Escherichia coli* K-12 in-frame, single-gene knockout mutants: the Keio collection. Mol Syst Biol **2:**2006.0008.

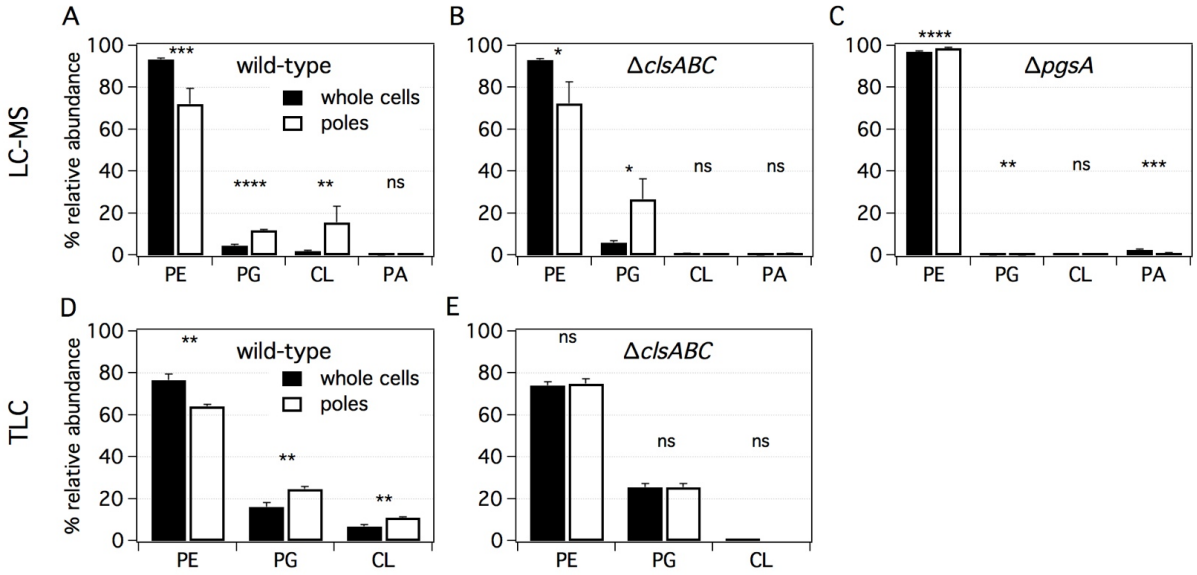

Figure S4. Relative abundances of PE, PG, CL, and PA determined by LC-MS (A-C) and TLC/phosphorus analysis (D & E) of minicell producing mutants of (A & D) wild-type (WM1032), (B & E) Δ *clsABC* (POM10), and (C) Δ *pgsA* (UEM543) *E. coli*. To assess differences between the lipid abundances in whole cells and poles in the various *E. coli* strains, we performed Chi-squared tests. All tests were two-sided and statistical significance was considered when a p-value < 0.05 was observed (ns, non-significant; *, $p < 0.05$; **, $p < 0.01$; ***, $p < 0.001$). Error bars indicate the standard deviation of the mean (n = 4+ replicates).

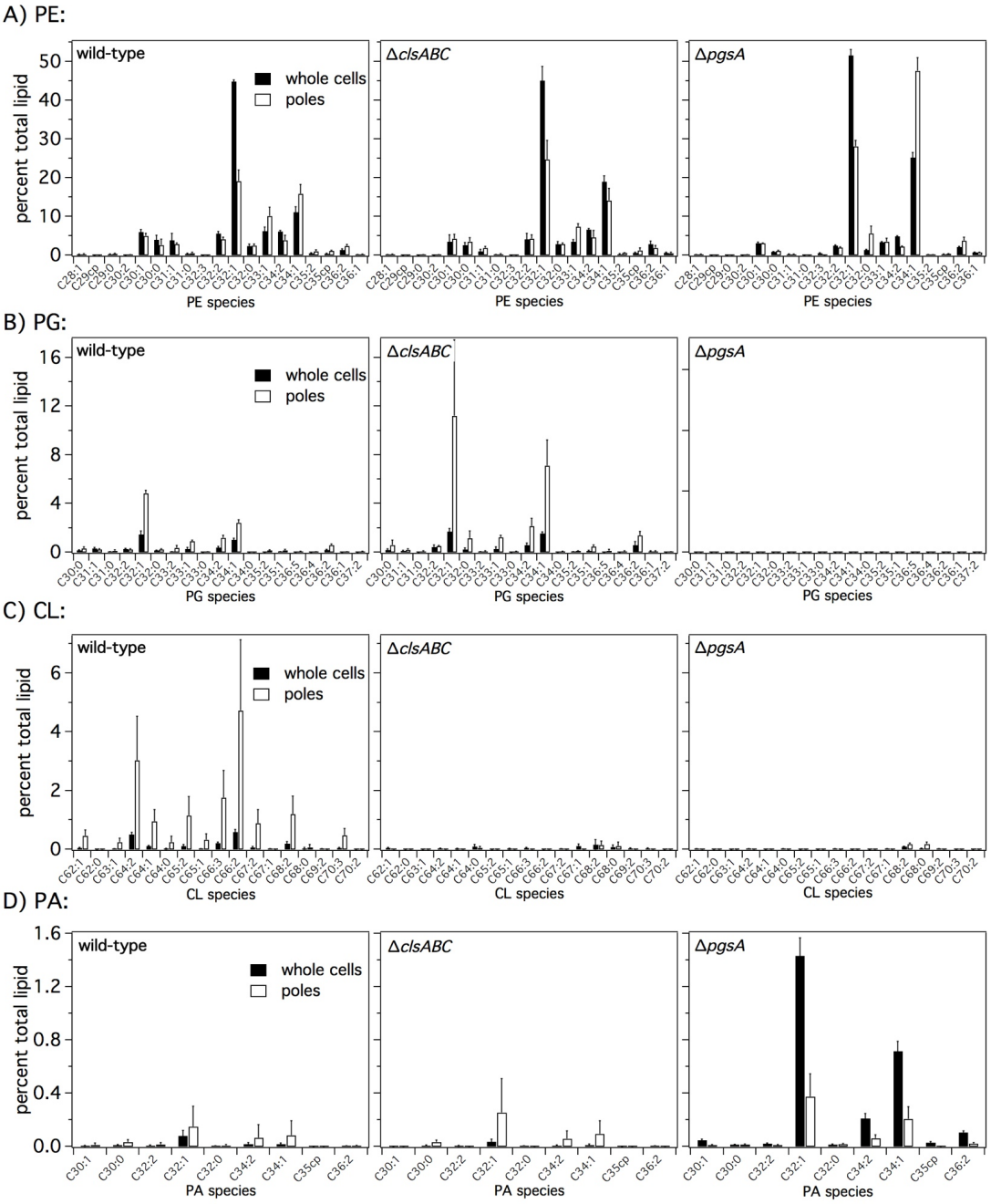

Figure S5. Fractional abundances of lipid species by LC-MS in whole cells and poles of the wild-type (WM1032), Δ *clsABC* (POM10), and Δ *pgsA* (UEM543) mutants of *E. coli*. Lipid species that were analyzed with respect to a corresponding internal standard are presented in this figure: (A) PE, (B) PG, (C) CL, and (D) PA. Each lipid species is presented as the total number of carbons in all alkyl chains on a PL, the total number of unsaturated bonds (after the colon), and whether or not a cyclopropyl group is present (i.e., "cp"). Error bars indicate the standard deviation of the mean (n = 4+ replicates). The fractional abundance of each species was calculated by dividing the average standardized intensity of one species by the average standardized summed total of all lipid species for all headgroups (i.e., PEs + PGs + CLs + PAs) for either whole cells or poles.

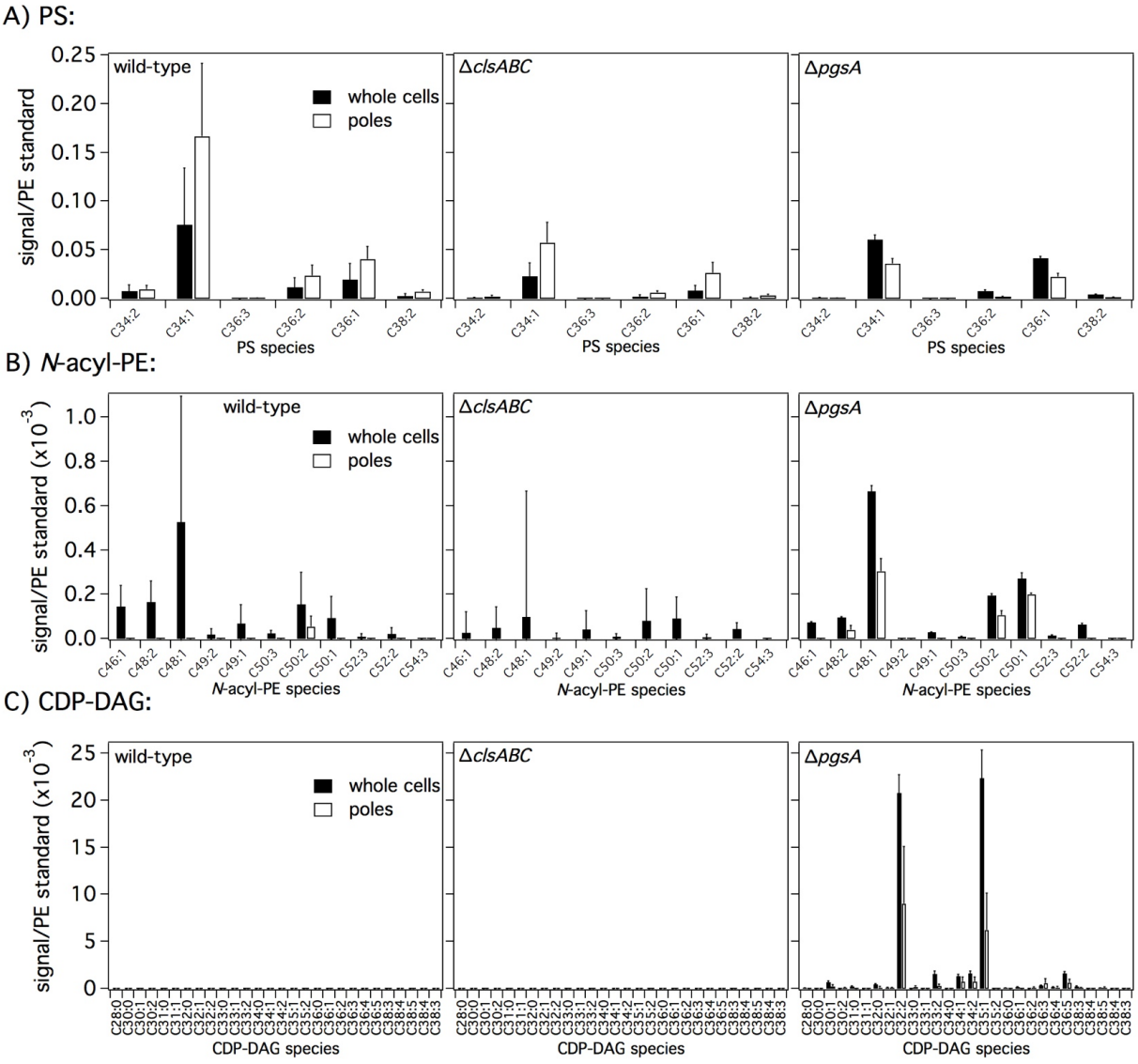

Figure S6. Semi-standardized intensities of lipid species by LC-MS in whole cells and poles of the wild-type (WM1032), Δ *clsABC* (POM10), and Δ*pgsA* (UEM543) mutants of *E. coli*. Lipid species that were not analyzed with respect to a corresponding internal standard are presented in this figure: (A) PS, (B) *N*-acyl-PE, and (C) CDP-DAG. Each lipid species is presented as the total number of carbons in all alkyl chains on a PL and the total number of unsaturated bonds (after the colon). Error bars indicate the standard deviation of the mean (n = 4+ replicates). The intensity of each species was calculated by dividing the average intensity of one species by the average summed total of all standardized lipid species (e.g., PEs + PGs + CLs + PAs) for either whole cells or poles. Since standards for PS, *N*-acyl-PE, and CDP-DAG were not added, relative comparisons can be made only within one family of lipids.

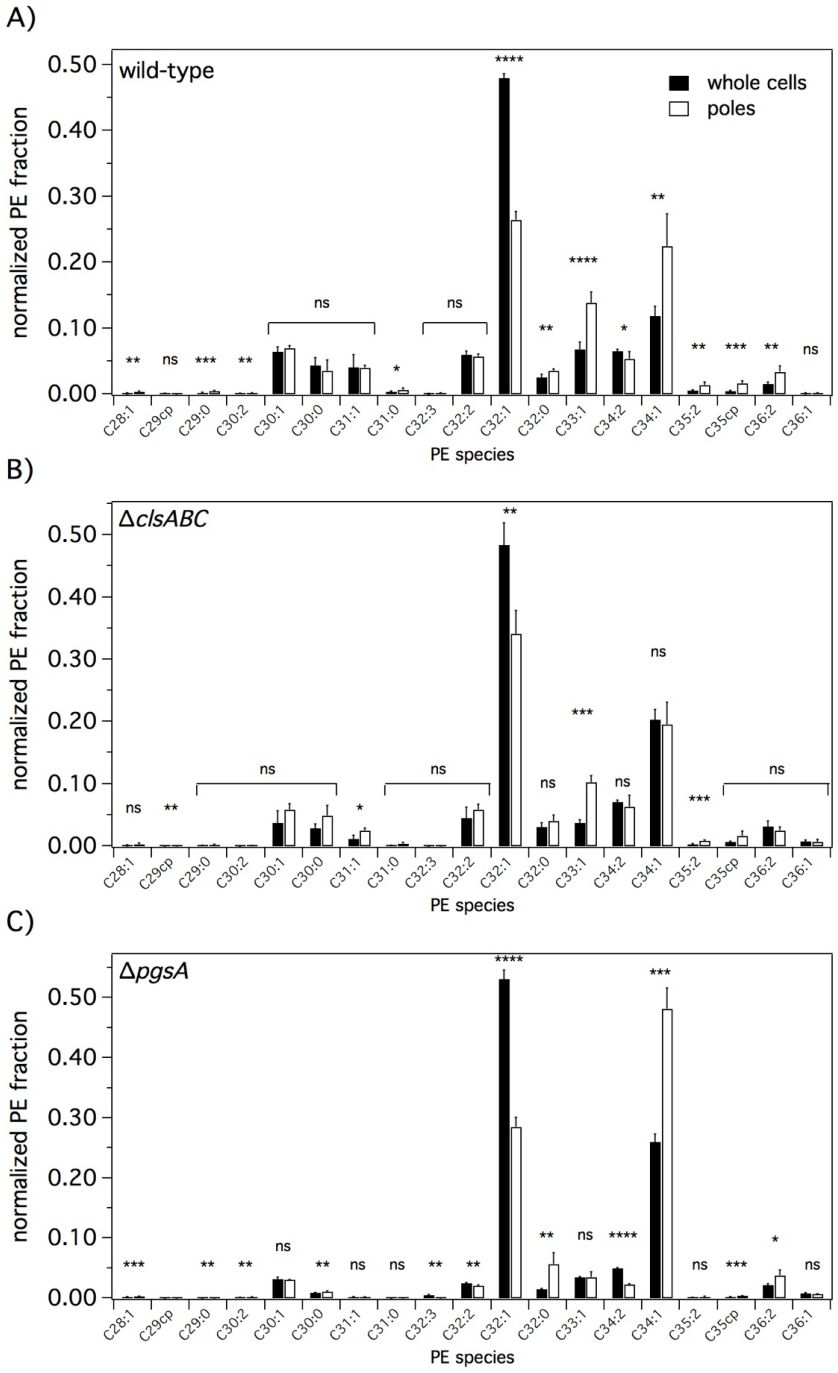

Figure S7. Normalized intensities of PE species by LC-MS in whole cells and poles of the A) wild-type (WM1032), B) Δ *clsABC* (POM10), and C) Δ *pgsA* (UEM543) mutants of *E. coli*. Intensities were normalized so that all the intensities of PE species for a particular mutant (whole cells or poles) sum to '1'. This comparison is independent of standards and other lipids. To assess differences between the lipid species abundances in whole cells and poles in the various *E. coli* strains, we performed Chi-squared tests. All tests were two-sided and statistical significance was considered when a p-value < 0.05 was observed (ns, non-significant; *, $p < 0.05$; **, $p < 0.01$; ***, $p < 0.001$). Error bars indicate the standard deviation of the mean (n = 4+ replicates).

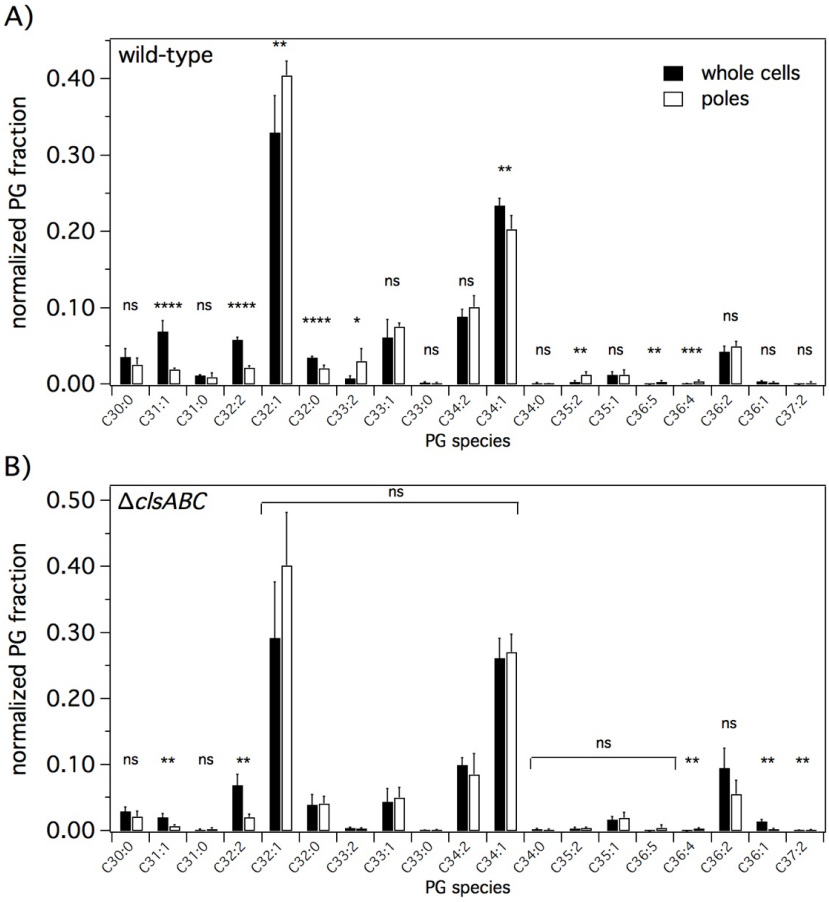

Figure S8. Normalized intensities of PG species by LC-MS in whole cells and poles of the A) wild-type (WM1032) and B) Δ *clsABC* (POM10) mutants of *E. coli*. The Δ*pgsA* (UEM543) mutant is not shown due to its low measured abundance of PGs. Intensities were normalized so that all the intensities of PG species for a particular mutant (whole cells or poles) sum to '1'. This comparison is independent of standards and other lipids. To assess differences between the lipid species abundances in whole cells and poles in the various *E. coli* strains, we performed Chi-squared tests. All tests were two-sided and statistical significance was considered when a p-value < 0.05 was observed (ns, non-significant; *, $p < 0.05$; **, $p < 0.01$; ***, $p < 0.001$). Error bars indicate the standard deviation of the mean (n = 4+ replicates).

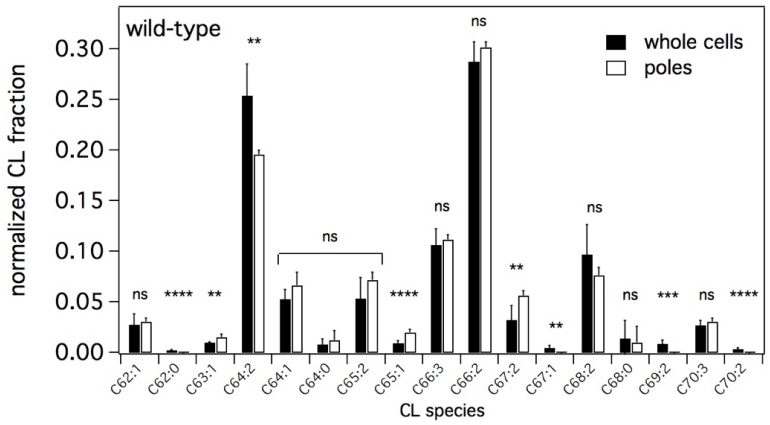

Figure S9. Normalized intensities of CL species by LC-MS in whole cells and poles of the wild-type (WM1032) *E. coli*. The Δ *clsABC* (POM10) and Δ*pgsA* (UEM543) mutants are not shown due to their low measured abundance of CLs. Intensities were normalized so that all the intensities of CL species for a particular mutant (whole cells or poles) sum to '1'. This comparison is independent of standards and other lipids. To assess differences between the lipid species abundances in the whole cells and poles in the *E. coli* strain, we performed Chi-squared tests. All tests were two-sided and statistical significance was considered when a p-value < 0.05 was observed (ns, non-significant; *, $p < 0.05$; **, $p < 0.01$; ***, $p < 0.001$). Error bars indicate the standard deviation of the mean (n = 4+ replicates).

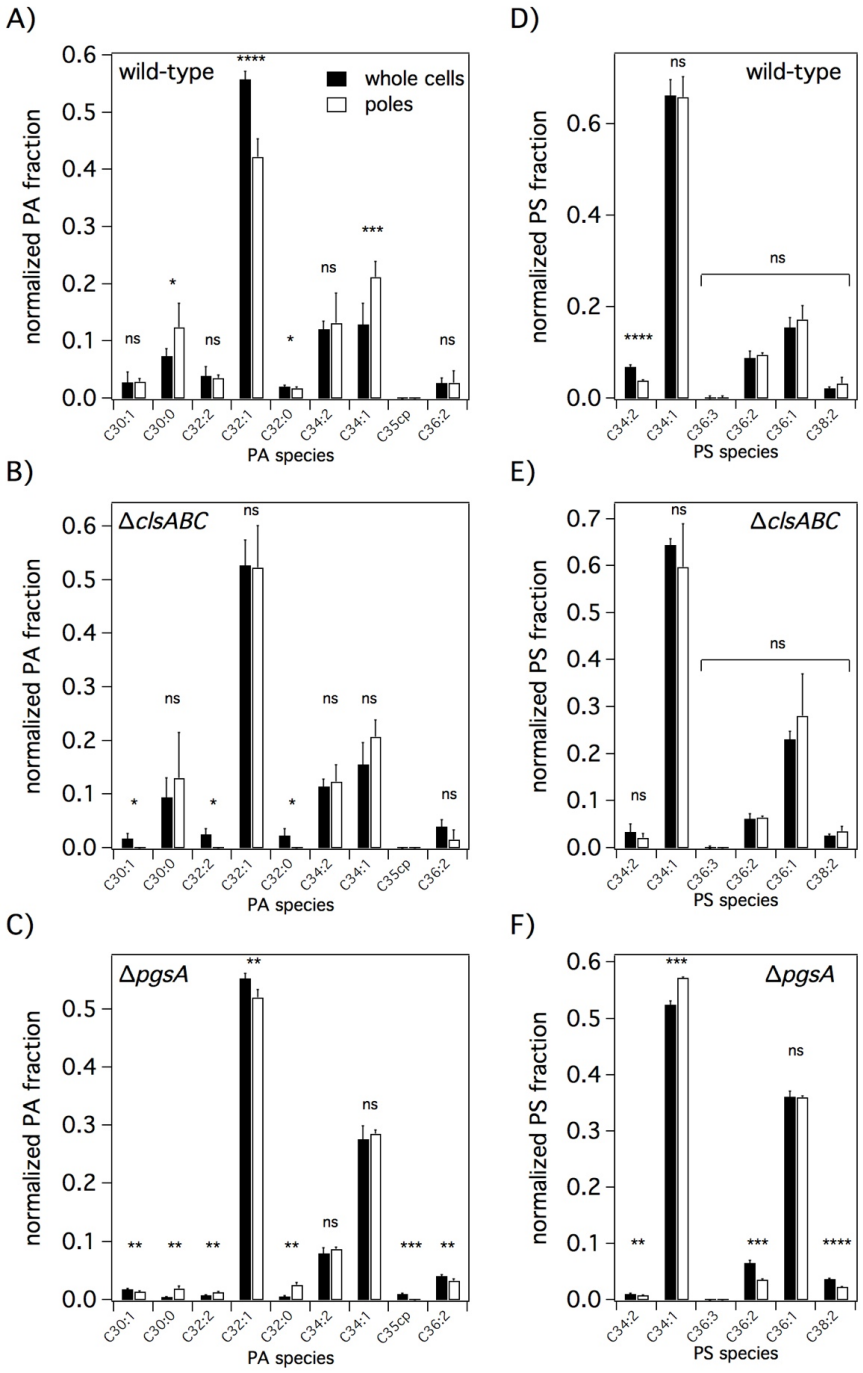

Figure S10. Normalized intensities of PA and PS species by LC-MS in whole cells and poles of the A & D) wild-type (WM1032), B & E) Δ*clsABC* (POM10), and C & F) Δ*pgsA* (UEM543) mutants of *E. coli*. Intensities were normalized so that all the intensities of PA or PS species for a particular mutant (whole cells or poles) sum to '1'. This comparison is independent of standards and other lipids. To assess differences between the lipid species abundances in whole cells and poles in the various *E. coli* strains, we performed Chi-squared tests. All tests were two-sided and statistical significance was considered when a p-value < 0.05 was observed (ns, non-significant; *, $p < 0.05$; **, $p < 0.01$; ***, $p < 0.001$). Error bars indicate the standard deviation of the mean (n = 4+ replicates).

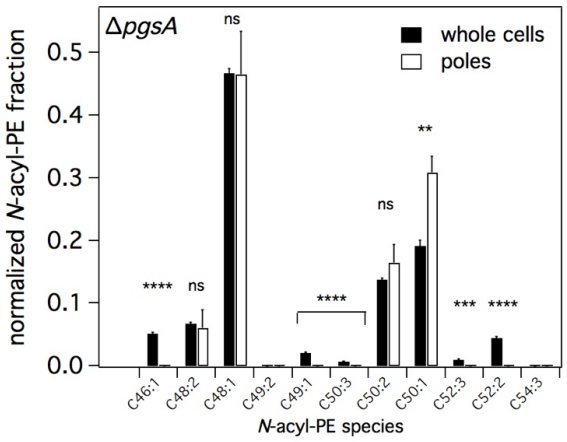

Figure S11. Normalized intensities of *N*-acyl-PE species by LC-MS in whole cells and poles of the Δ*pgsA* (UEM543) mutant of *E. coli*. The wild-type (WM1032) and Δ*clsABC* (POM10) mutants are not shown due to their low measured abundance of *N*-acyl-PEs. Intensities were normalized so that all the intensities of *N*-acyl-PE species for a particular mutant (whole cells or poles) sum to '1'. This comparison is independent of standards and other lipids. To assess differences between the lipid species abundances in whole cells and poles in the *E. coli* strain, we performed Chi-squared tests. All tests were two-sided and statistical significance was considered when a p-value < 0.05 was observed (ns, non-significant; *, $p < 0.05$; **, $p < 0.01$; ***, $p < 0.001$). Error bars indicate the standard deviation of the mean (n = 4 replicates).

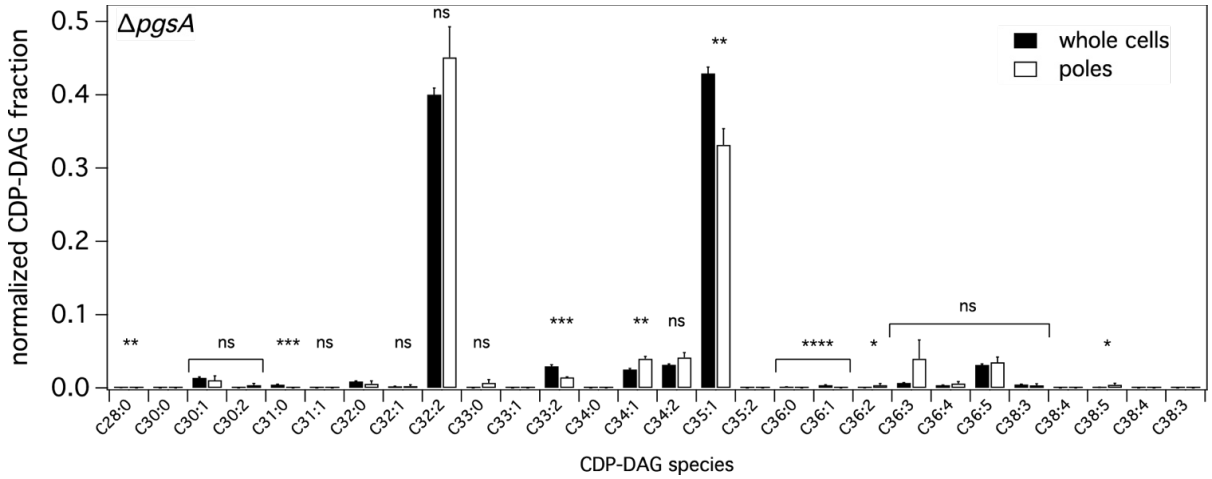

Figure S12. Normalized intensities of CDP-DAG species by LC-MS in whole cells and poles of the Δ*pgsA* (UEM543) mutant of *E. coli*. The wild-type (WM1032) and Δ*clsABC* (POM10) mutants are not shown due to their low measured abundance of CDP-DAGs. Intensities were normalized so that all the intensities of CDP-DAG species for a particular mutant (whole cells or poles) sum to '1'. This comparison is independent of standards and other lipids. To assess differences between the lipid species abundances in whole cells and poles in the *E. coli* strain, we performed Chi-squared tests. All tests were two-sided and statistical significance was considered when a p-value < 0.05 was observed (ns, non-significant; *, $p < 0.05$; **, $p < 0.01$; ***, $p < 0.001$). Error bars indicate the standard deviation of the mean (n = 4 replicates).

Table S1. Semi-standardized total intensities (arbitrary units) of lipid species PS, *N*-acyl-PE, and CDP-DAG by LC-MS in whole cells and poles of the wild-type (WM1032), Δ*clsABC* (POM10), and Δ*pgsA* (UEM543) mutants of *E. coli*. Each of these total lipid species was normalized to the average summed total of all standardized lipid species (e.g., PEs + PGs + CLs + PAs) for either whole cells or poles. Since standards for PS, *N*-acyl-PE, and CDP-DAG were not added, comparisons can only be made within one family of lipids. To assess differences between the lipid abundances in whole cells and poles in the various *E. coli* strains, we performed Chi-squared tests. All tests were two-sided and statistical significance was considered when a p-value < 0.05 was observed (ns, non-significant; *, $p < 0.05$; **, $p < 0.01$; ***, $p < 0.001$).

	PS			***N*-acyl-PE**			**CDP-DAG**		
Genotype	**Whole cells**	***p***	**Poles**	**Whole cells**	***p***	**Poles**	**Whole cells**	***p***	**Poles**
Wild-type	0.12 (±0.09)	*	0.2 (±0.1)	1 (±1)×10^{-3}	*	60 (±50)×10^{-6}	*n.d.*		*n.d.*
Δ*clsABC*	0.04 (±0.02)	*	0.10 (±0.03)	0.5 (±0.1)×10^{-3}		*n.d.*	*n.d.*		*n.d.*
Δ*pgsA*	0.116 (±0.007)	***	0.063 (±0.009)	1.42 (±0.06)×10^{-3}	****	0.65 (±0.06)×10^{-3}	52 (±6)×10^{-3}	**	20 (±12)×10^{-3}

"*n.d.*" = none detected

Table S2. Molecular mass of PE and PG species detected in *E. coli*. Each lipid species is presented as the total number of carbons in all alkyl chains on a PL, the total number of unsaturated bonds (after the colon), and whether or not a cyclopropyl group is present (i.e., "cp").

PE acyl chain compositions	PE mass		PG acyl chain compositions	PG mass	
	Exact	Measured		Exact	Measured
Carbons:unsaturations	*[M-H]⁻*		*Carbons:unsaturations*	*[M-H]⁻*	
C28:1	632.4291	632.4304	C30:0	693.4722	693.4710
C29cp*	646.4448	676.4909	C31:1	705.4729	705.4711
C29:0	648.4627	648.4621	C31:0	707.4870	707.4863
C30:2	658.4448	658.4456	C32:2	717.4725	717.4710
C30:1	660.4620	660.4604	C32:1	719.4873	719.4889
C30:0	662.4776	662.4765	C32:0	721.5039	721.5025
C31:1	674.4779	674.4797	C33:2	731.4887	731.4883
C31:0	676.4917	676.4909	C33:1	733.5030	733.5048
C32:3	684.4604	684.4596	C33:0	735.5211	735.5198
C32:2	686.4776	686.4794	C34:2	745.5034	745.5018
C32:1	688.4930	688.4915	C34:1	747.5188	747.5191
C32:0	690.5080	690.5080	C34:0	749.5311	749.5342
C33:1	702.5074	702.5066	C35:2	759.5147	759.5179
C34:2	714.4985	714.5073	C35:1	761.5358	761.5337
C34:1	716.5244	716.5257	C36:5	767.4891	767.4848
C35:2	728.5230	728.5222	C36:4	769.5046	769.5000
C35cp*	730.5387	730.5372	C36:2	773.5327	773.5330
C36:2	742.5361	742.5393	C36:1	775.5489	775.5494
C36:1	744.5551	744.5547	C37:2	787.5510	787.5493

* "cp" designates that one of the fatty acids is cyclopropanated

Table S3. Molecular mass of CL and PA species detected in *E. coli*. Each lipid species is presented as the total number of carbons in all alkyl chains on a PL, the total number of unsaturated bonds (after the colon), and whether or not a cyclopropyl group is present (i.e., "cp")

CL acyl chain compositions		CL mass		PA acyl chain compositions	PA mass	
		Exact	Measured		Exact	Measured
Carbons:unsaturations	*Most likely structure*[2]	*[M-H]*$^-$		*Carbons:unsaturations*	*[M-H]*$^-$	
C62:1	C16:1/C16:0 C16:0/C14:0	1321.9180	1321.9278	C30:1	617.4182	617.4183
C62:0	C16:0/C16:0 C16:0/C14:0	1323.9337	1323.9492	C30:0	619.4339	619.4348
C63:1	C17:1/C16:0 C16:0/C14:0	1335.9337	1335.9443	C32:2	643.4339	643.4349
C64:2	C16:1/C16:0 C16:1/C16:0	1347.9341	1347.9453	C32:1	645.4495	645.4520
C64:1	C16:1/C16:0 C16:0/C16:0	1349.9491	1349.9624	C32:0	647.4652	647.4608
C64:0	C16:0/C16:0 C16:0/C16:0	1351.9491	1351.9736	C34:2	671.4660	671.4664
C65:2	C17:1/C16:0 C16:1/C16:0	1361.9491	1361.9601	C34:1	673.4808	673.4842
C65:1	C17:1/C16:0 C16:0/C16:0	1363.9650	1363.9760	C35cp*	687.4965	687.4959
C66:3	C18:1/C16:1 C16:1/C16:0	1373.9501	1373.9585	C36:2	699.4965	699.4944
C66:2	C18:1/C16:0 C16:1/C16:0	1375.9640	1375.9739			
C67:2	C18:1/C16:0 C17:1/C16:0	1389.9801	1389.9921			
C67:1	C18:0/C16:0 C17:1/C16:0	1391.9801	1392.0046			
C68:2	C18:1/C16:0 C18:1/C16:0	1403.9961	1404.0076			
C68:0	C18:0/C16:0 C18:0/C16:0	1408.0271	1408.0362			
C69:2	C18:0/C16:1 C18:0/C17:1	1418.0119	1418.0227			
C70:3	C18:1/C16:0 C18:1/C18:1	1430.0121	1430.0185			
C70:2	C18:1/C16:1 C18:0/C18:0	1432.0276	1432.0319			

* "cp" designates that one of the fatty acids is cyclopropanated

[2] Hsu, F. F., & Turk, J. (2006). Characterization of cardiolipin from Escherichia coli by electrospray ionization with multiple stage quadrupole ion-trap mass spectrometric analysis of [M−2H+Na]− ions. *Journal of the American Society for Mass Spectrometry*, *17*(3), 420–429. doi:10.1016/j.jasms.2005.11.019

Table S4. Molecular mass of PS and *N*-acyl-PE species detected in *E. coli*. Each lipid species is presented as the total number of carbons in all alkyl chains on a PL and the total number of unsaturated bonds (after the colon).

PS acyl chain compositions	**PS mass**		***N*-acyl-PE acyl chain compositions**[3]	***N*-acyl-PE mass**	
	Exact	**Measured**		**Exact**	**Measured**
Carbons:unsaturations	*[M-H]⁻*		*Carbons:unsaturations*	*[M-H]⁻*	
C34:2	758.4955	758.4984	C46:1	898.690	898.6899
C34:1	760.5143	760.5145	C48:2	924.706	924.7060
C36:3	784.5138	784.5141	C48:1	926.721	926.7226
C36:2	786.5298	786.5299	C49:2	938.721	938.7218
C36:1	788.5459	788.5462	C49:1	940.737	940.7370
C38:2	814.5604	814.5598	C50:3	950.721	950.7196
			C50:2	952.737	952.7360
			C50:1	954.753	954.7522
			C52:3	978.753	978.7499
			C52:2	980.768	980.7689
			C54:3	1006.780	*n.d.*

[3] Mileykovskaya, E., Ryan, A., Mo, X., Lin, C., Khalaf, K., Dowhan, W., & Garrett, T. (2009). Phosphatidic acid and *N*-acylphosphatidylethanolamine form membrane domains in Escherichia coli mutant lacking cardiolipin and phosphatidylglycerol. *The Journal of Biological Chemistry*, *284*(5), 2990–3000.

Table S5. Molecular mass of CDP-DAG species detected in *E. coli*. Each lipid species is presented as the total number of carbons in all alkyl chains on a PL and the total number of unsaturated bonds (after the colon).

CDP-DAG acyl chain compositions	CDP-DAG mass	
	Exact	Measured
Carbons:unsaturations	*[M-H]⁻*	
C28:0	896.4439	896.4408
C30:0	920.4439	*n.d.*
C30:1	922.4595	922.4599
C30:2	924.4752	924.4759
C31:0	936.4752	936.4713
C31:1	938.4908	*n.d.*
C32:0	948.4752	948.4759
C32:1	948.4752	948.4738
C32:2	950.4908	950.4913
C33:0	952.5065	952.5057
C33:1	962.4908	*n.d.*
C33:2	964.5065	964.5048
C34:0	966.5221	*n.d.*
C34:1	976.5065	976.5069
C34:2	976.5065	976.5070
C35:1	978.5221	978.5239
C35:2	980.5378	*n.d.*
C36:0	990.5221	990.5188
C36:1	992.5378	992.5344
C36:2	998.4908	998.4892
C36:3	1000.5065	1000.5035
C36:4	1002.5221	1002.5165
C36:5	1004.5378	1004.5376
C38:3	1006.5534	1006.5518
C38:4	1008.5691	*n.d.*
C38:5	1026.5221	1026.5222
C38:4	1028.5378	*n.d.*
C38:3	1030.5534	*n.d.*